Coastal Engineering 179 (2023) 104249

Contents lists available at ScienceDirect

Coastal Engineering

journal homepage: www.elsevier.com/locate/coastaleng

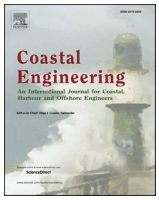

A reduced-complexity shoreline model for coastal areas with large water level fluctuations

Hazem U. Abdelhady *, Cary D. Troy

Purdue University, Lyles School of Civil Engineering, 550 Stadium Mall Drive, West Lafayette, IN, 47907-2051, USA

ARTICLE INFO

Keywords:
Shoreline model
Shoreline changes
Water level fluctuations
Lake Michigan
Shoreline equilibrium
Great Lakes
Satellite images
Remote sensing
Coastal changes

ABSTRACT

A new reduced-complexity, 1-D shoreline model has been developed, calibrated, and tested with a set of shoreline positions detected from high-resolution satellite images. Motivated by recent large interannual water level fluctuations and associated shoreline changes in the Great Lakes, the model is built on previous models that are based on the disequilibrium concept, with extensions for water level effects. Unlike other shoreline models, the model includes two different sources of disequilibrium, wave disequilibrium and water level disequilibrium. The model also includes a passive flooding term to account for the instantaneous effect of the water level changes on the shoreline position. Case studies forced by seasonally-varying waves and water levels varying on seasonal and interannual timescales highlight the model's ability to enhance wave-driven shoreline change when water level variations are additionally present. The model was applied to two sites along the Lake Michigan shoreline, Jeorse Park and West Beaches, with shoreline time series extracted from multispectral satellite imagery. When calibrated and applied to an eleven year period of decreasing water levels, the new model shows significant skill in simulating and forecasting the shoreline position in the two study areas, with modest improvement over existing models. The simulation results additionally highlight the dominance of water level disequilibrium over wave disequilibrium for the study sites. When applied to a nearly forty year simulation of West Beach, the new model shows excellent ability to model the shoreline response to water level and wave fluctuations over a range of timescales. Comparison models are seen to be incapable of capturing the water level effects, particularly when water level trends differ from the calibration period. Overall, the model results and parameters show the importance of the newly introduced water level disequilibrium in modulating wave-driven shoreline change. Finally, while the shoreline model was motivated by Great Lakes coastal processes, it may provide new predication abilities for coastlines where water level fluctuations and trends play a role in shoreline changes.

1. Introduction

Beach geomorphology change is driven by complex hydrodynamic processes with a wide range of time scales (Pape et al., 2010; Payo et al., 2016). Although waves are thought to be the main driver of the changes in beach geomorphology at shorter time scales (Davidson et al., 2013; Yates et al., 2009), water level fluctuations and trends also play an important role in beach reshaping (Alauddin Al Azad et al., 2018; Coco et al., 2014; D'anna et al., 2021). On event timescales, storm surge communicates wave energy to more erodible portions of the beach, enhancing shoreline erosion (Alauddin Al Azad et al., 2018; Coco et al., 2014). On decadal and longer timescales, sea level rise leads to shoreline recession as the beach profile recedes to retain its equilibrium (e.g., the Bruun Rule (Bruun, 1962)).

In the Great Lakes, such as Lake Michigan, water level fluctuations play a key role in beach dynamics on both short and long timescales (Fig. 1) (Theuerkauf et al., 2019; Thompson and Baedke, 1995). Great Lakes water level fluctuations differ in several ways from ocean coasts, with important consequences for beach response. On sub-daily to weekly timescales, most ocean coastlines experience tidal forcing, and this high-frequency shoreline scrubbing creates wider beaches, and beaches that are in quasi-equilibrium with a larger range of water levels (Friedrichs, 2011; Masselink and Short, 1993). In contrast, the Great Lakes have negligible tidal influence, which in turn means that beaches

Abbreviations: GLSM, Great Lakes Shoreline Model; USGS, United States Geological Survey; USACE, United States Army Corps of Engineers; WIS, Wave Information Study; LiDAR, Light Detection and Ranging.

* Corresponding author.
E-mail address: abdelhah@purdue.edu (H.U. Abdelhady).

https://doi.org/10.1016/j.coastaleng.2022.104249
Received 7 July 2022; Received in revised form 5 October 2022; Accepted 5 November 2022
Available online 9 November 2022

are generally narrower, and more narrowly tuned to the water levels, which means that the beach response is more strongly dependent on the water level fluctuations that do occur on seasonal and interannual timescales.

On seasonal, interannual, and decadal timescales, the Great Lakes experience much larger water level fluctuations than ocean coasts (Fig. 1). These fluctuations are driven by hydrologic variations on a wide range of timescales (Gronewold and Rood, 2019), and while it has not been shown that the Great Lakes water levels are experiencing long-term trends analogous to sea level rise, recent work suggests that climate change may lead to increased interannual variability in water levels, resulting from the tug of war between increasing precipitation and increasing evaporation (Gronewold and Rood, 2019). Between 2013 and 2020, for example, the Lake Michigan-Huron water level went from a record low to a record high, with the lake shorelines experiencing a water level increase of approximately 2 m over seven years (Fig. 1). This water level increase was felt across the Great Lakes, with extensive shoreline damage resulting from the rapid increase (Theuerkauf et al., 2019; Troy et al., 2021).

In essence it may be argued that Great Lakes coasts are dually disadvantaged when it comes to the erosive effect of rising water levels on shorelines. Firstly, the magnitudes of longer-term (seasonal scale and beyond) water level fluctuations in the Great Lakes are much larger than those experienced along ocean coasts. But secondly, the lack of short-term water level fluctuations (like tides) in the Great Lakes means that the beaches are in equilibrium with only a very small range of water levels at any instant in time, in turn making them even more susceptible to the large, lower frequency Great Lakes water level variations. It is for these reasons that we hypothesize that the water level plays a much more important role in Great Lakes beach morphodynamics than for ocean coastlines, which is supported by recent observations (Theuerkauf et al., 2019; Troy et al., 2021).

Reduced complexity shoreline position models have been developed and applied with success to simulate the cross-shore movement of the shoreline in response to wave forcing. These models aim to resolve shoreline changes resulting from wave-driven cross-shore sediment transport (Davidson et al., 2013; Miller and Dean, 2004; Splinter et al., 2014; Yates et al., 2009), alongshore sediment transport (Ashton and Murray, 2006; Hanson, 1989; Vitousek and Barnard, 2015), or a combination of the two mechanisms (Antolínez et al., 2019; Robinet et al., 2018; Tran and Barthélemy, 2020; Vitousek et al., 2017). Many of the modern cross-shore shoreline models are based on the disequilibrium concepts introduced by Wright and Short (1984), where the beach response to wave forcing at an instant in time is a function of the

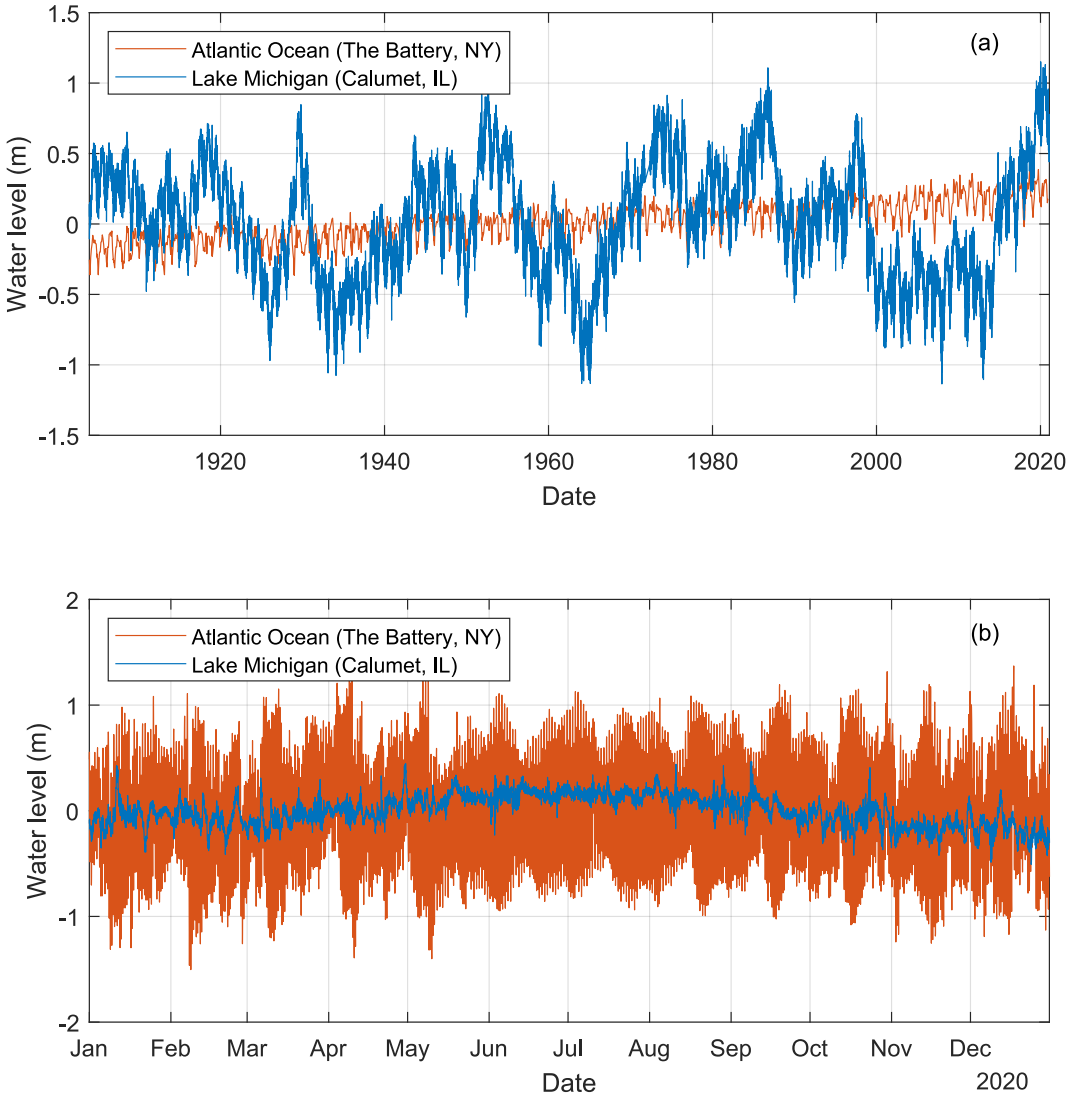

Fig. 1. (a) Monthly water level fluctuations for Lake Michigan and the Atlantic Ocean from 1904 to 2020. (b) Hourly water level fluctuations for Lake Michigan and the Atlantic Ocean for the year 2020. Data extracted from NOAA Gages 9087044 and 8518750 for Lake Michigan and the Atlantic Ocean respectively (https://tidesandcurrents.noaa.gov/waterlevels).

difference, or disequilibrium, from recent beach and/or wave conditions. Inherently the dis/equilibrium modeling concept assumes that the beach morphology is in equilibrium with recent wave conditions, as defined by an appropriate timescale, and stronger deviations from these recent conditions lead to a stronger beach response to wave forcing. Metrics of wave disequilibrium used in these models include wave energy (Yates et al., 2009) and the dimensionless fall velocity (Davidson et al., 2013; Splinter et al., 2014).

When calibrated, reduced-complexity equilibrium shoreline models have been shown to successfully simulate wave-driven shoreline changes for many coastlines (Davidson et al., 2013; Ibaceta et al., 2020; Miller and Dean, 2004; Muir et al., 2020; Splinter et al., 2014; Robinet et al., 2017, 2018; Schepper et al., 2021; Tran and Barthélemy, 2020; Vitousek and Barnard, 2015; Vitousek et al., 2017). While full morphological models account for water level changes explicitly (Lesser et al., 2004; Roelvink et al., 2009), reduced complexity shoreline models generally do not take into account water level variations, and thus any shoreline movement affected by water level changes are effectively aliased into the wave forcing terms in the models. It is not surprising or even a shortcoming that water level effects are not considered in most reduced-complexity shoreline models, since to date applications have been restricted to ocean coasts on shorter timescales. On ocean coasts, as described earlier, water level fluctuations are dominated by high-frequency tidal variations, which at sub-daily timescales are not resolved with the typical daily simulation step used in these models.

The modeling of water level effects on shoreline position has thus far been focused on two limiting timescales. At one end of the spectrum, the effects of rapid, short-term water level fluctuations on shoreline position such as tides or storm surge can be modeled as "passive" beach flooding or exposure, as outlined by Vitousek et al. (2017). In this passive flooding limit, water simply moves up or down the passive, unmoving beach face, and horizontal shoreline movement is reasonably assumed to be proportional to the beach slope at the water's edge (typically 1/10 or so).

The opposite timescale limit is the long-term shoreline recession associated with sea level rise, which has traditionally been modeled with the Bruun Rule (Bruun, 1962). In this long-term limit, shoreline recession is again assumed to be proportional to a beach slope, but in this case the effective beach slope dictating recession is the overall slope of the entire active profile, from the onshore berm to the offshore depth of closure (typically 1/90-1/800; these numbers are corresponding to the 75 and 25 percentiles respectively presented by Athanasiou et al. (2019). The Bruun Rule effectively assumes that the recessed beach profile maintains equilibrium with the water level, and preserves the profile shape starting from the intersection point of the profile with the water level seaward.

In related, recent work, we showed that the magnitude of the recent Lake Michigan beach response to the seasonal and interannual water level increases is somewhere between these two limits, with an effective recession slope of approximately 1/30 (Troy et al., 2021). Measurements of the geomorphic response along seven Lake Michigan beaches by Theuerkauf et al. (2019) revealed that the key variable that differentiated the geomorphic response of the beaches was the change in water levels. This finding suggests that the beach erosion process for the Great Lakes is not well-described by either limit or model, likely due to the magnitude and frequency of the water level fluctuations as described earlier, and the lack of equilibrium between changing water levels and the actively evolving beach profile over seasonal and interannual timescales.

The objective of the present study is to develop and test a simplified shoreline model that successfully captures the effects of rapid, large seasonal and interannual water level changes on shoreline change, which we believe is an important lacking model feature that hinders the application of existing models to Great Lakes shorelines. Through analogy to how wave effects are modeled in existing shoreline models, the proposed model is based on the concept of "water level disequilibrium", where low-frequency water level fluctuations enhance wave-driven shoreline changes. The model is tested on two shorelines along southern Lake Michigan that have recessed extensively between 2013 and 2020 in response to high water levels, and compared to existing reduced-complexity models that do not model water level effects.

2. Model development

2.1. Model formulation

The proposed "Great Lakes Shoreline Model" (GLSM) proposed here is similar in overall structure to the existing ShoreFor model (Splinter et al., 2014), with modifications to account for water level effects. The model formulation for the daily change in cross-shore shoreline position with time is

$$\frac{dy}{dt} = \left(\overbrace{F^{+}}^{(1)} + r\overbrace{F^{-}}^{(2)} \right) + \overbrace{\frac{C_{pf}}{\tan(\alpha)}\frac{dS}{dt}}^{(3)} + \overbrace{b}^{(4)} \tag{1}$$

Here $\frac{dy}{dt}$ is the time rate of change of the shoreline position in the cross-shore direction, with $\frac{dy}{dt} > 0$ implying shoreline advancement, and $\frac{dy}{dt} < 0$ implying shoreline recession. Terms 1 and 2 represent wave driven shoreline advancement and retreat, respectively, with shoreline change being proportional to wave energy, modulated by wave and water level disequilibrium (described in detail below). The dimensionless constant r accounts for differences between accretion and the erosion response rates to wave forcing, following previous modeling (Davidson et al., 2013; Miller and Dean, 2004; Splinter et al., 2014; Yates et al., 2009). Term 3 in Equation (1) represents the effect of passive flooding and exposure due to water level changes (dS/dt) on the shoreline position, where $\tan(\alpha)$ represents the average cross-shore slope of the beach face at the waterline and C_{pf} is the passive flooding constant, a free dimensionless parameter, following Vitousek et al. (2017). This passive flooding term (Term 3) accounts for simple geometric inundation and exposure as the water level rises and falls and the shoreline advances and recedes, respectively. The constant C_{pf} is an O(1) constant introduced to account for the uncertainty associated with the spatial and temporal variability in beach foreshore slopes. The linear term b (Term 4) is introduced in the model to account for all other unresolved long-term processes such as alongshore transport gradients, following previous work (Davidson et al., 2013; Vitousek et al., 2017).

The broad formulation of the wave-driven shoreline change terms F^{+} (shoreline advancement) and F^{-} (shoreline recession) is the same as the ShoreFor model, namely

$$F = P^{0.5}\frac{\Delta A}{\sigma_{\Delta A}} \tag{2}$$

with $F = F^{+}$ when ΔA is positive (advancement), and $F = F^{-}$ when ΔA is negative (recession). Here P is the deep water incident wave power estimated with linear wave theory:

$$P = \frac{1}{16}\rho g H^{2} C_{g} \tag{3}$$

where H is the wave height, ρ is the water density, g is gravity, and C_g represents the group velocity.

The term $\Delta A/\sigma_{\Delta A}$ is the normalized, dimensionless disequilibrium term in the model, and is calculated as

$$\Delta A = A_{eq} - A \tag{4}$$

Where A is the physical variable defining equilibrium, A_{eq} is its equilibrium value (typically taken as a weighted average of recent values over a defined timescale), and $\sigma_{\Delta A}$ is the standard deviation of the whole timeseries of A, which captures the regular variability of the system.

The equilibrium value A_{eq} is calculated as a weighted average of the previous A factors over a duration of 2 φ days following the same weighting factors suggested by Splinter et al. (2014).

$$A_{eq} = \frac{\sum_{i=1}^{2\varphi} A_i 10^{-i/\varphi}}{\sum_{i=1}^{2\varphi} 10^{-i/\varphi}} \tag{5}$$

Here i represents the number of days prior to the present time and φ represents the response factor for the modeled shoreline.

Previous models, focused on wave disequilibrium as the primary variable that modulates wave-driven shoreline changes, have defined A with the dimensionless fall velocity:

$$A = A_H = \frac{H}{WT} \tag{6}$$

Where H is the wave height, W is a representative sediment fall velocity, and T is the wave period. The general interpretation of the dimensionless fall velocity is that high values are associated with erosive conditions, and lower values cause shoreline growth (Wright and Short, 1984). With A_H as the equilibrium variable in (4), wave-driven shoreline recession is enhanced by events with relatively large values of A_H, relative to a weighted average of recent values A_{eq} over a time period $2\varphi_H$, i.e. the disequilibrium $\Delta A/\sigma_A$. Conversely, low values of the dimensionless fall velocity, relative to the equilibrium (recent) values, cause shoreline advancement.

To additionally account for enhanced shoreline changes resulting

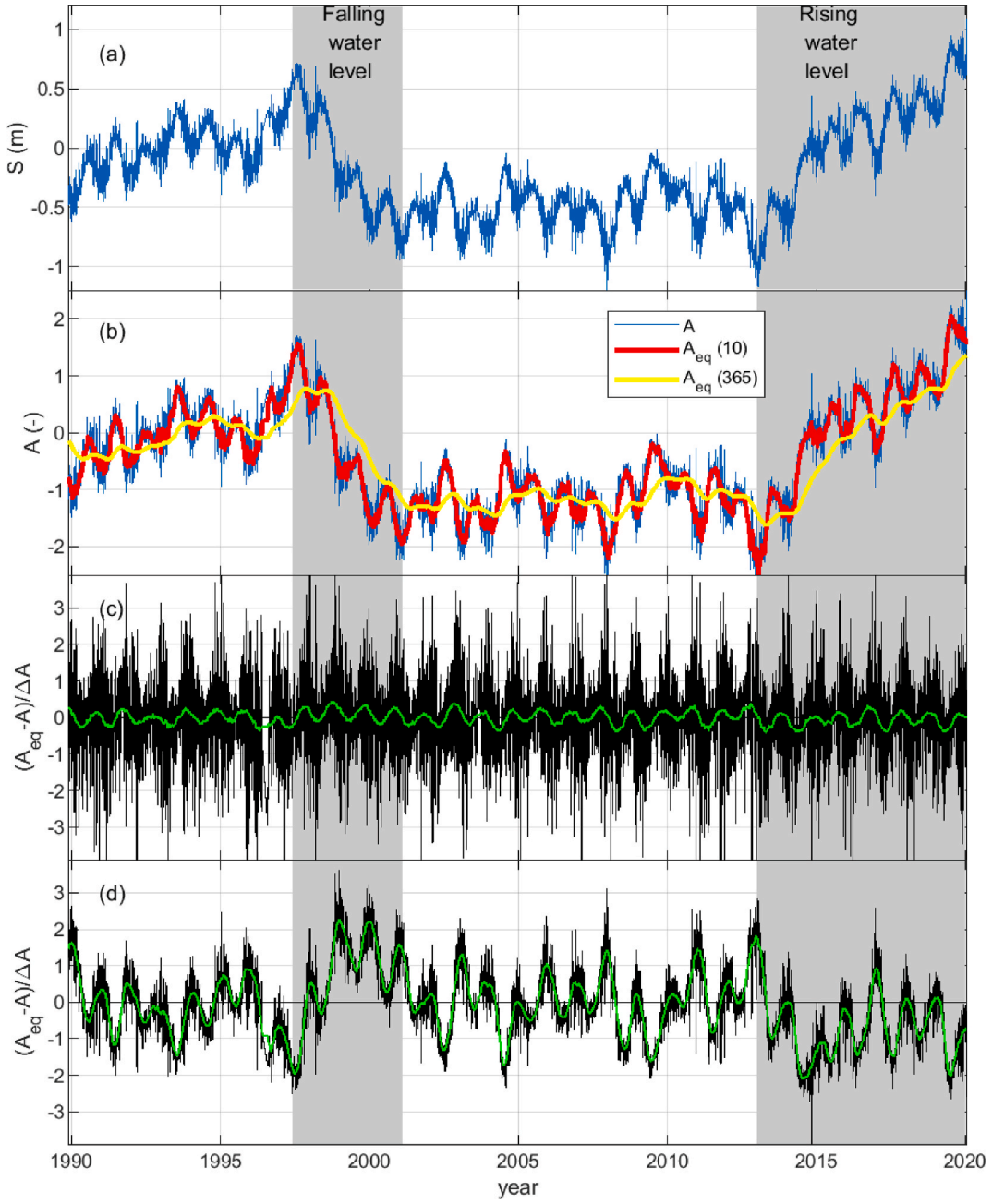

Fig. 2. Illustration of water level disequilibrium term. Shown are (a) Lake Michigan water levels, relative to long-term mean; (b) dimensionless water level A_S and equilibrium water level A_{eq} calculated with φ_S = 183 days and 365 days; (c) resulting water level disequilibrium term (raw and smoothed) for φ_S = 10 days; (d) resulting water level disequilibrium term (raw and smoothed) for φ_S = 365 days.

from beach disequilibrium caused by sustained, appreciable water level changes, we introduce a water level disequilibrium variable A_S:

$$A_S = \frac{S}{\sigma_S} \tag{7}$$

Here S is the instantaneous (daily average) water level relative to a long-term mean or datum, and σ_S is the standard deviation of S over the period of record. The equilibrium value of A_S is taken as a weighted average of water level values (S) over a timescale $2\varphi_S$ that reflects the timescale required for the shoreline to respond to water level changes.

An illustration of how the water level disequilibrium term functions is shown in Fig. 2. Two periods of longer-term water level changes are highlighted. For the falling water level period of the years 1997–2001, the equilibrium water level consistently exceeds the actual water level, leading to a positive disequilibrium term, Equation (4). This positive disequilibrium term for falling water levels then serves to enhance wave-driven shoreline advancement via Equation (2). The opposite is true for rising water levels (2013–2020), where the equilibrium water level is generally less than the actual (rising) water level, in turn leading to a negative disequilibrium term that will lead to wave-enhanced shoreline recession.

We define the total disequilibrium as the sum of the wave and water level disequilibrium, as

$$\frac{\Delta A}{\sigma_{\Delta A}} = C_H \frac{\Delta A_H}{\sigma_{\Delta A_H}} + C_S \frac{\Delta A_S}{\sigma_{\Delta A_S}} \tag{8}$$

Here the weighting constants C_H and C_S are introduced in order to provide system-specific weightings for the relative and absolute importance of wave- and water level-driven disequilibrium in causing shoreline changes. With $C_{pf} = 0$ and $C_S = 0$, the model reverts to the popular ShoreFor model (Splinter et al., 2014).

2.2. Synthetic test cases

To illustrate the behavior of the water level disequilibrium mechanism, two idealized, synthetic cases of water level and wave forcing were examined and solved numerically ("Case 1" and "Case 2"). For wave forcing, both cases are forced with seasonally-varying wave conditions that mimic the average wave variability seen in Lake Michigan with large waves in winter and smaller waves in summer. For water level forcing, Case 1 isolates the model response to low-frequency, interannual water level changes; Case 2 has seasonal variations in water level

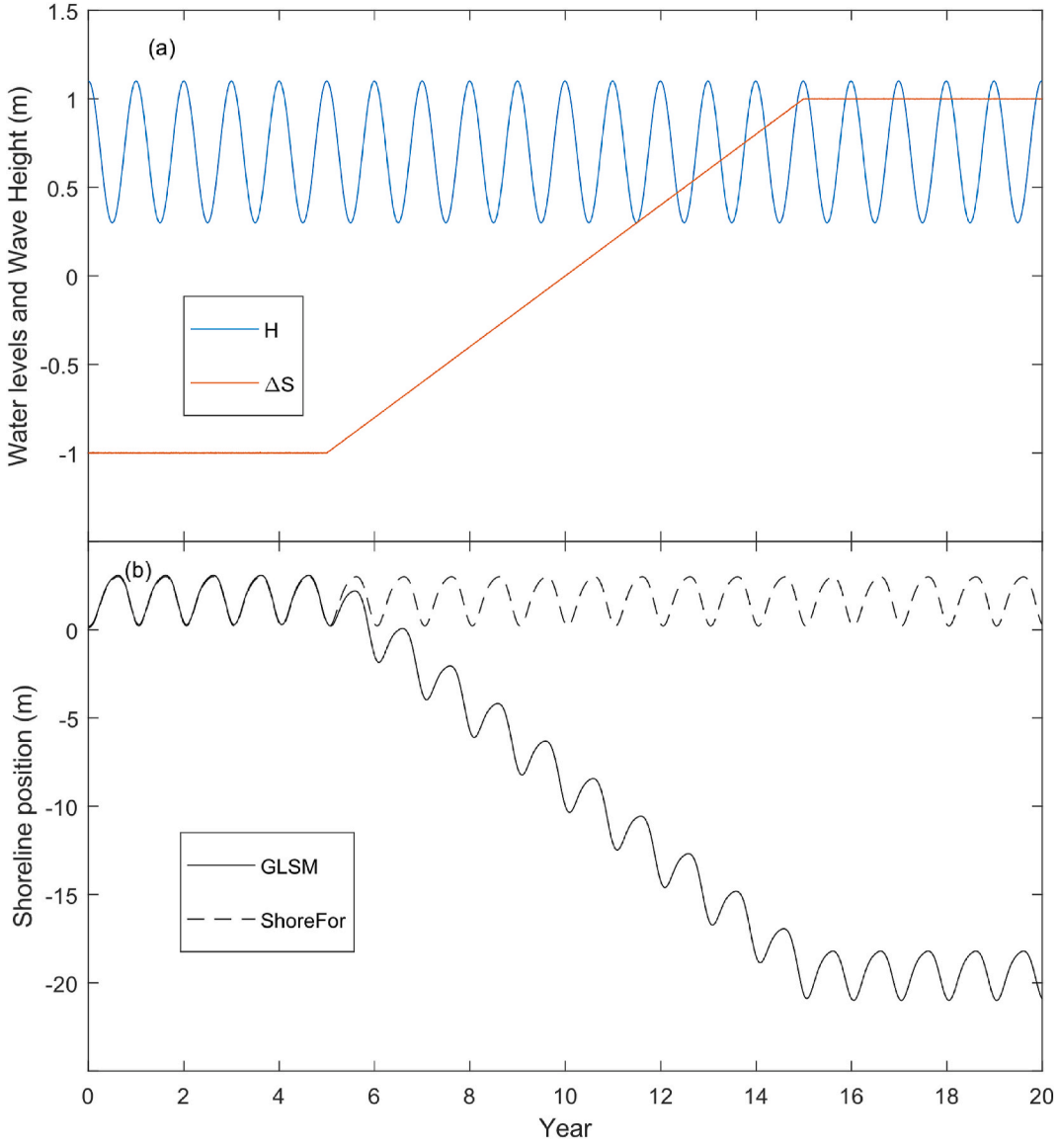

Fig. 3. Synthetic Case 1. Panel (a) shows wave height and water level forcing; Panel (b) shows the GLSM and ShoreFor model responses.

on top of the Case 1 interannual water level changes. The seasonally-varying Case 2 water levels are maximum in summer and minimum in winter, which means that they are phase shifted from the seasonal wave pattern by half of a year (this pattern is also the usual pattern in Lake Michigan).

For Case 1, the wave height was varied sinusoidally over an annual cycle with largest wave heights in the fall and the winter and smallest wave heights in the spring and the summer (Fig. 3). The water level in Case 1 was taken to be constant for the first 5 years of the simulation, then linearly increased 2 m over a period of 10 years, followed by a constant high-water level for the remainder of the simulation. This water level increase mimics the recent observed low-frequency interannual cycle of water level increase in Lake Michigan from 2013 to 2020 (Fig. 1).

Because the purpose of the synthetic test cases was to highlight modeling behavior associated with the addition of the water level disequilibrium term (Equation (1)), the passive flooding (Term 3) was not used for the synthetic test cases (i.e. Term 3 was set to 0). For both cases, models' parameters were selected to produce a magnitude of shoreline movement response roughly comparable to what has been observed in Lake Michigan for a good visual comparison between the two models (Table 1). The model was coded in MATLAB (MATLAB, 2019) and solved with a direct Euler scheme with a daily timestep. The simplified model without passive flooding was also solved without the water level disequilibrium term, for which the simplified model reverts to the ShoreFor model as mentioned previously (Splinter et al., 2014).

The simplified model responses to Case 1 are shown in Fig. 3, with and without the inclusion of the water level disequilibrium term. With no water level changes in the first 5 years of the simulation, both models produce the same lagged periodic response to the seasonally-varying wave heights. The simplified GLSM model with the water level disequilibrium term, however, produces shoreline retreat in response to the increase in the water levels. As expected, the baseline ShoreFor model responds to the seasonally-varying waves but not the interannual water level changes, since water level effects are not included in the model.

For Case 2, the simplified GLSM and ShoreFor shoreline responses differ throughout the simulation period, including the period where the water level does not vary interannually (Fig. 4). The Case 2 ShoreFor response is identical to the Case 1 response. During the first five years of the simulation, both models produce a periodic shoreline response, but for Case 2 the two models are phase shifted relative to one another, since the simplified GLSM solution is additionally responding to the seasonally-varying water levels. This phase lag is particular to the model coefficients used in the simulations (Table 1). The GLSM is seen to again respond to the interannual water level fluctuations in a physically-realistic manner, similar to the Case 1 response.

Table 1
Model coefficients used for the synthetic case studies.

Parameters	Case 1	Case 2
GLSM		
C_H ($m^{1.5}/day^{-1}/W^{-0.5}$)	0.00050	0.0006
C_S ($m^{1.5}/day^{-1}/W^{-0.5}$)	0.00015	0.0011
φ_S (days)	72	72
φ_H (days)	72	72
b (m/day)	0.00364	−0.0030
C_{pf}	0	0
r	0.10	0.10
ShoreFor		
C ($m^{1.5}/day^{-1}/W^{-0.5}$)	0.00050	0.00050
b (m/day)	0.00364	0.00364
φ (days)	72	72
r	0.10	0.10

3. Model application

3.1. Study area

The main study location for this work is the Indiana coastline of Lake Michigan (USA; Fig. 5). Lake Michigan is the second largest Great Lake by volume and the third largest by area (Bockheim, 2020). Lake Michigan coasts are considered nontidal, but experience annual average water level fluctuations of ± 0.15 m due to seasonal variations in the hydrologic cycle. As discussed previously, Lake Michigan water levels exhibit large variations on a range of longer timescales (Cheng et al., 2021; Hanrahan et al., 2009) (Fig. 1). The lake experiences the largest wind waves in the fall and winter (Mortimer, 2004), with maximum significant wave heights of 5–6 m and maximum wave periods of 12–13 s (Feng et al., 2020; Melby et al., 2012). The dominant direction of sediment drift along the Indiana coastline is towards the southwest, with several large harbors acting as littoral barriers that separate the coastline into distinct coastal cells (Fig. 5).

This study focused on two Indiana Lake Michigan shoreline sites: (1) Jeorse Park Beach (1.6 km long); and (2) Marquette Park Beach and West Beach (hereafter jointly referred to as West Beach; 5.6 km long). The shorelines examined here are primarily comprised of fine sandy beaches backed by vegetated dunes, with shoreline use being primarily recreational. The median sediment sizes for the dry portions of Jeorse and West Beaches are 0.26 and 0.33 mm respectively, which was determined using a standard sieve analysis carried out on collected samples. The foreshore beach slopes of Jeorse and West Beach were estimated as 1/16 and 1/19, respectively, using 2012 USACE/NOAA topo-bathymetric LiDAR data. While the two beaches are separated by only 13 km, waves at Jeorse Park Beach are largely diminished relative to West Beach due to the presence of the large, 4 km long Indiana Harbor that blocks waves from the northwest.

In related recent work, we developed an automated procedure to extract shoreline positions and discern shoreline changes from newly available commercial high-resolution multispectral satellite images (Abdelhady et al., 2022). This algorithm was applied in the present work to construct a high temporal and spatial resolution timeseries for the shoreline positions for the two study locations, using the Planetscope and RapidEye satellites (Figs. 6 and 7) (Planetscope). Planetscope imagery is available from early 2016 to present, and RapidEye imagery is available from 2009 to 2019. The average revisit time for the Planetscope and RapidEye satellites are 1 and 5.5 days respectively. The extracted time series for the two shorelines presented in this study are shown in Figs. 6 and 7. In all 171 shoreline positions for West Beach were extracted for the period 2009 to 2019, and 264 shoreline positions for Jeorse Park Beach were extracted for the period 2009 to 2019. Gaps present in the time series are due to the presence of cloud cover and shore ice. The estimated uncertainty in the shoreline positions is estimated to be equal to half the pixel size of the images (Abdelhady et al., 2022) (±1.5 m for the Planetscope images and ±2.5 m for the Rapideye images).

In addition to the high-frequency shoreline position time series derived from the Planetscope and RapidEye satellite imagery, available older aerial and satellite imagery was utilized to determine discrete historical shoreline positions for the beaches for the period 1987–2008, for longer model runs described in the Discussion section.

Hourly wave descriptors near both shorelines were extracted from the U.S. Wave Information Study (WIS) simulation from stations 94005 and 94001 for Jeorse Park Beach and West Beach respectively, for the period 1979–2019 (U.S. Army Corps of Engineers, 2022). These stations are located approximately 6.9 km and 6.8 km from the beaches, in 11 m and 17 m depth water, respectively (Fig. 5).

3.2. Model calibration

The optimization of the free parameters was done using an optimi-

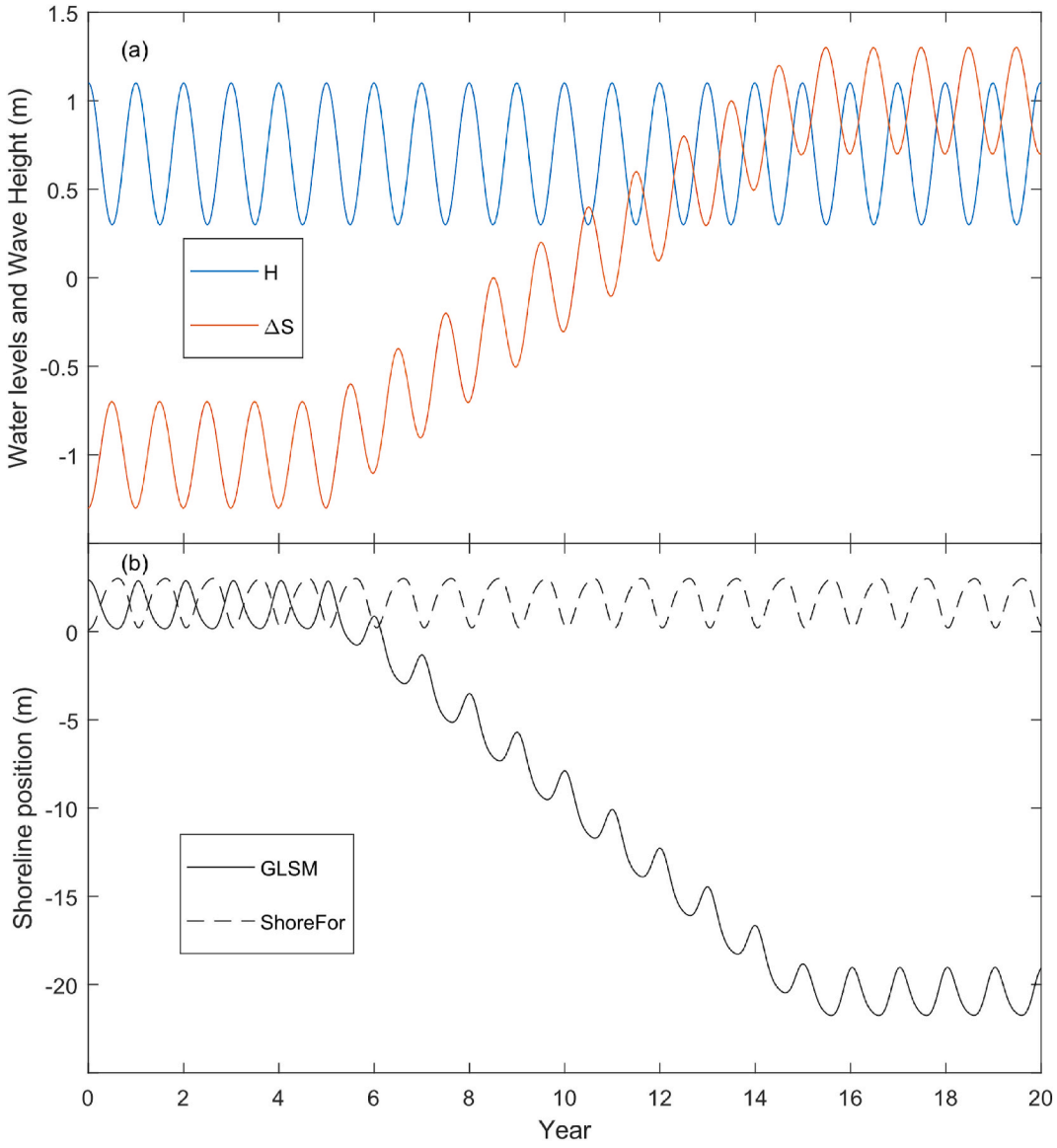

Fig. 4. Synthetic Case 2. Panel (a) shows wave height and water level forcing; Panel (b) shows the GLSM and ShoreFor modeled shoreline position responses.

zation algorithm that included least squares optimization and a genetic algorithm. A direct least squares optimization for equation (1) was not possible due to the presence of the C_H, C_S, φ_S and φ_H parameters that are embedded into the model factors and need to be constrained. Thus, a genetic algorithm (Katoch et al., 2021) was used as an outer loop to change these four parameters while in each loop the optimum values for the C_{pf} and b are determined using the least squares optimization. This technique was found to be faster and more robust than using the genetic algorithm for all the parameters. The genetic algorithm was chosen due to its ability to deal efficiently with the mixed integer optimization problems (Deep et al., 2009).

The model was calibrated on the data available from 2009 to the end of 2017. The two years 2018–2019 were left for the model to forecast (i.e. validate). A daily timestep was used for model calculations. The maximum hourly wave height for each day and the corresponding peak wave period were used for calculations of the wave energy and the dimensionless fall velocity, while the average daily water levels were used for the water levels term.

The ShoreFor model proposed by Splinter et al. (2014) was used as a reference model for comparison. This model was selected for comparison because the GLSM is an extension to that model, and because the ShoreFor model does not account for the influence of water levels on shoreline positions and thus provides an interesting baseline case against which the proposed model can be compared. The proposed GLSM simulations were also compared to solutions produced from a shoreline model containing only the passive flooding term (Term 3 in Equation (1)). The calibration of the comparison models was done using the least squares optimization as suggested by Davidson et al. (2013) and Splinter et al. (2014).

3.3. Model skill evaluation and comparison

The proposed GLSM simulations were compared to solutions produced from the ShoreFor model equations, with two metrics used to assess the performance of the model and to compare the model skill with existing models. The first metric was the root mean square error (RMSE) between the model and the observations.

The second metric was the Brier Skill Score (BSS) (Sutherland and Soulsby, 2003). The advantage of this metric is that it allows the comparison of performance between two models. The form of the BSS used in this study is:

Fig. 5. Study area at southern Lake Michigan (satellite imagery courtesy of Esri, DigitalGlobe, GeoEye, Earthstar Geographics, CNES/Airbus DS, USDA, USGS, AeroGRID, IGN, and the GIS User Community).

$$BSS = 1 - \frac{\sum (y - y_m)^2}{\sum (y - y_r)^2} \tag{9}$$

Positive values for the BSS indicate that the proposed model (y_m) is an improvement over the reference model (y_r), with values exceeding 0, 0.3, 0.6, 0.8 considered as poor, fair, good, and excellent improvement, respectively, according to (Davidson et al., 2013; Splinter et al., 2014). Negative values indicate that the proposed model does not improve over the reference model.

4. Results

4.1. Jeorse Park beach

Simulation results for Jeorse Park Beach are shown in Fig. 8, with optimized calibration parameters provided in Table 2. When calibrated, both models are able to simulate the observed shoreline changes with very good accuracy. The full GLSM has root mean square errors in the simulated shoreline position of 1.85 m and 1.48 m for the hindcast and forecast periods (i.e. calibration and validation), respectively, with corresponding ShoreFor values of 2.74 m and 2.48 m for the same periods. Both models are able to capture the lower-frequency interannual variability in the shoreline position correctly for the relatively constant shoreline position during the period of constant water level (2009–2013), and producing a retreating shoreline during the period of rising water level (2013–2019). The character of the two solutions differs with respect to the high frequency of the shoreline response; the GLSM is seen to have larger fluctuations in the shoreline position on daily to weekly timescales.

When evaluated for improvement, the GLSM showed good improvement over a linear trend, and the improvement provided by the ShoreFor model over the linear trend model was evaluated to be poor (Table 3). Relative to one another, the GLSM was evaluated to have good improvement over the ShoreFor model for the Jeorse Park Beach simulation, which would be expected given that the latter model has no knowledge of the water level changes.

The optimized calibration coefficients for the two models provide insight into the different mechanisms by which both models capture the shoreline position (Table 2). The low wave disequilibrium coefficient value of $C_H = 6.22\text{x}10 - 8$ for the GLSM indicates that the water level disequilibrium term is the main factor modulating wave forcing, and that wave disequilibrium plays a negligible role in setting the shoreline position. When investigated further, it was found that the wave forcing term, although primarily modulated by water level disequilibrium, contributed to only a small amount of the shoreline changes simulated at Jeorse Park Beach, while the passive flooding term was found to be the primary mechanism responsible for the simulated changes. Thus, in spite of the potential complexity afforded by the water level disequilibrium mechanism that was introduced into the GLSM, the shoreline model effectively reverted to the simple passive flooding model (Term 3) introduced by Vitousek et al. (2017) for this beach. While not expected, this behavior makes sense in hindsight, because of the very low amount of wave energy that the beach experiences, due to its location south of the massive Indiana Harbor that effectively blocks waves from the west and most importantly the north, which is the direction of maximum fetch. It should be noted that the WIS wave station used for the Jeorse Park Beach modeling is likely not representative of the beach wave climate, due to its offshore location where the station lies outside of the

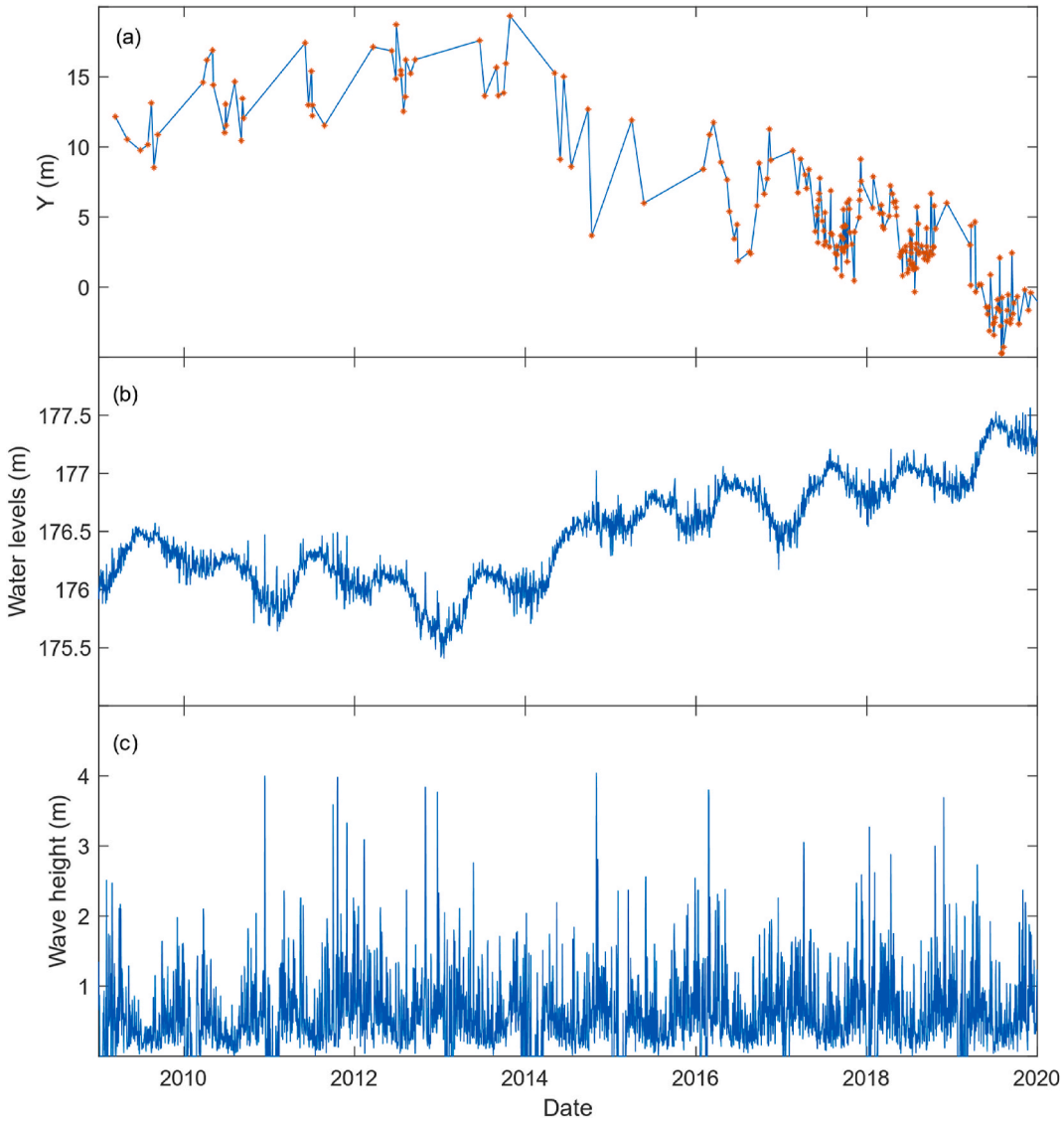

Fig. 6. (a) Average shoreline movement for Jeorse Park Beach, as inferred from satellite imagery (positive indicates advancement); (b) water level from 2009 to 2020 extracted from NOAA Gauge 9087044; (c) wave heights from WIS station 94005.

influence of the large harbor, as seen in Fig. 5. Thus, it seems reasonable that the primary mechanism causing shoreline changes at Jeorse Park Beach is simply passive flooding and exposure.

4.2. West Beach

For the West Beach simulations, both models show reasonable agreement with the low-frequency, interannual shoreline response, but the GLSM is seen to produce much more accurate shoreline positions on finer, sub-annual timescales. The RMSE values for West Beach simulations using the GLSM are 2.37 m and 2.35 m, for the hindcast and forecast periods (i.e. calibration and validation) respectively, and the optimized ShoreFor simulation results have respective RMSE values of 4.41 m and 4.43 m (Table 4). Model improvement metrics are rated excellent and good for the GLSM in comparison to linear trends, but only fair and poor for the ShoreFor model. When compared against each other, the GLSM shows good improvement over the ShoreFor model for both the calibration period (2009–2017) as well as the forecast period (2018–2019) (Table 4 and Fig. 9).

For the West Beach simulations, calibrated model parameters reveal that the water level term plays an important role in capturing the shoreline changes, which explains why the GLSM outperforms the ShoreFor model for this beach (Table 2). For the GLSM, the water level disequilibrium coefficient C_S is four orders of magnitude greater than the wave disequilibrium coefficient C_H, showing that the wave disequilibrium mechanism that typically drives ocean shoreline changes is not active at the West Beach site either (Table 2).

5. Discussion

The synthetic case studies and field applications of the proposed shoreline model (GLSM) highlight the model's ability to simulate shoreline changes enhanced and driven by the large, low-frequency water level fluctuations seen in the Great Lakes. The character of these water level fluctuations is unique to the Great Lakes and their effect on shoreline changes is not captured in existing reduced-complexity shoreline models. The GLSM introduced herein simulates water level effects on shoreline position via two mechanisms: (1) passive flooding (Term 3 in Equation (1)); and (2) the modulation of wave forcing via a water level disequilibrium mechanism (Equations (7) and (8)). Differences in the wave climate at the two beaches lead to differences in the relative importance of each mechanism, and the relative improvement

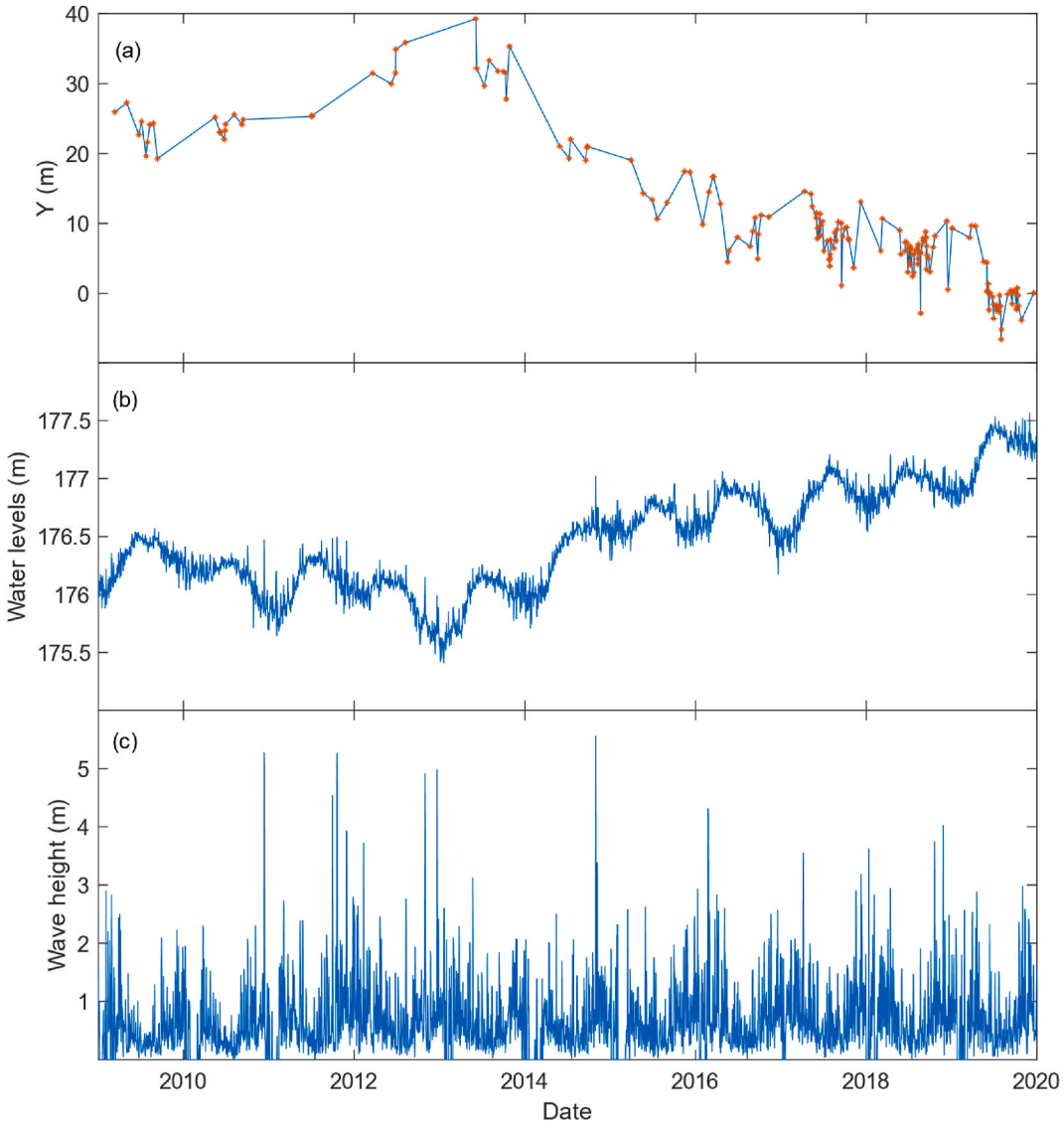

Fig. 7. (a) Average shoreline movement for West Beach, as inferred from satellite imagery; (b) water level from 2009 to 2020 extracted from NOAA Gauge 9087044; (c) wave heights from WIS station 94001.

provided by the new model.

At Jeorse Park Beach, which is strongly sheltered from wave energy, the passive flooding term in the model is able to capture most of the shoreline position variability over the period 2009–2019. The ShoreFor Model is also able to simulate the shoreline position well for Jeorse Park Beach, due to the aliasing of the passive flooding water level effect into the linear term in the model (Term 4 in Equation (1)). Overall, the GLSM shows a significant improvement over the linear trend and the ShoreFor models for Jeorse Beach.

At West Beach, which experiences the full power of Lake Michigan's large north-south fetch, the calibrated GLSM provides more substantial improvement in the shoreline position estimation, because there both passive flooding and water level disequilibrium are important mechanisms causing shoreline change. For this location, the GLSM provides more substantial improvement over the linear and ShoreFor models. The ShoreFor model is still able to simulate the shoreline position reasonably well for West Beach, with less than 5 m error, which again is presumably due to the aliasing of water level effects into the model's linear term b.

For the simulations shown of the 10-year periods, it may not appear that the increased complexity afforded by the new model is entirely warranted, given that the simulations without the water level terms still provide reasonable (<5 m RMSE) accuracy. However, as a first point, it could be noted that Great Lakes shoreline models should have a higher absolute shoreline position accuracy requirement, due to the much smaller beach widths and overall shoreline movements relative to ocean beaches.

More importantly, with no mechanism to account for water level effects, the ShoreFor model is succeeding in the two test cases by absorbing the effects of the changing water levels into the wave forcing and linear terms in the model. For example, the optimized linear term (b) in the ShoreFor model simulation is one order of magnitude larger than the corresponding GLSM values for both beaches. Additionally, for both locations, the optimized ShoreFor wave forcing coefficients (C) are negative, which is not physically plausible (the optimization is not constrained). Again, this is not a shortcoming of the ocean-focused ShoreFor model, because the oceans do not face the magnitude and duration of the large Great Lakes water level fluctuations, it is merely instructive. While the two-year (2018–2019) validation period used in the simulations presented herein do provide some independent validation of the calibrated model, this period has a very similar water level trend to the calibration period (2009–2017), and therefore the linear shoreline trend term can effectively predict the future (2018–2019).

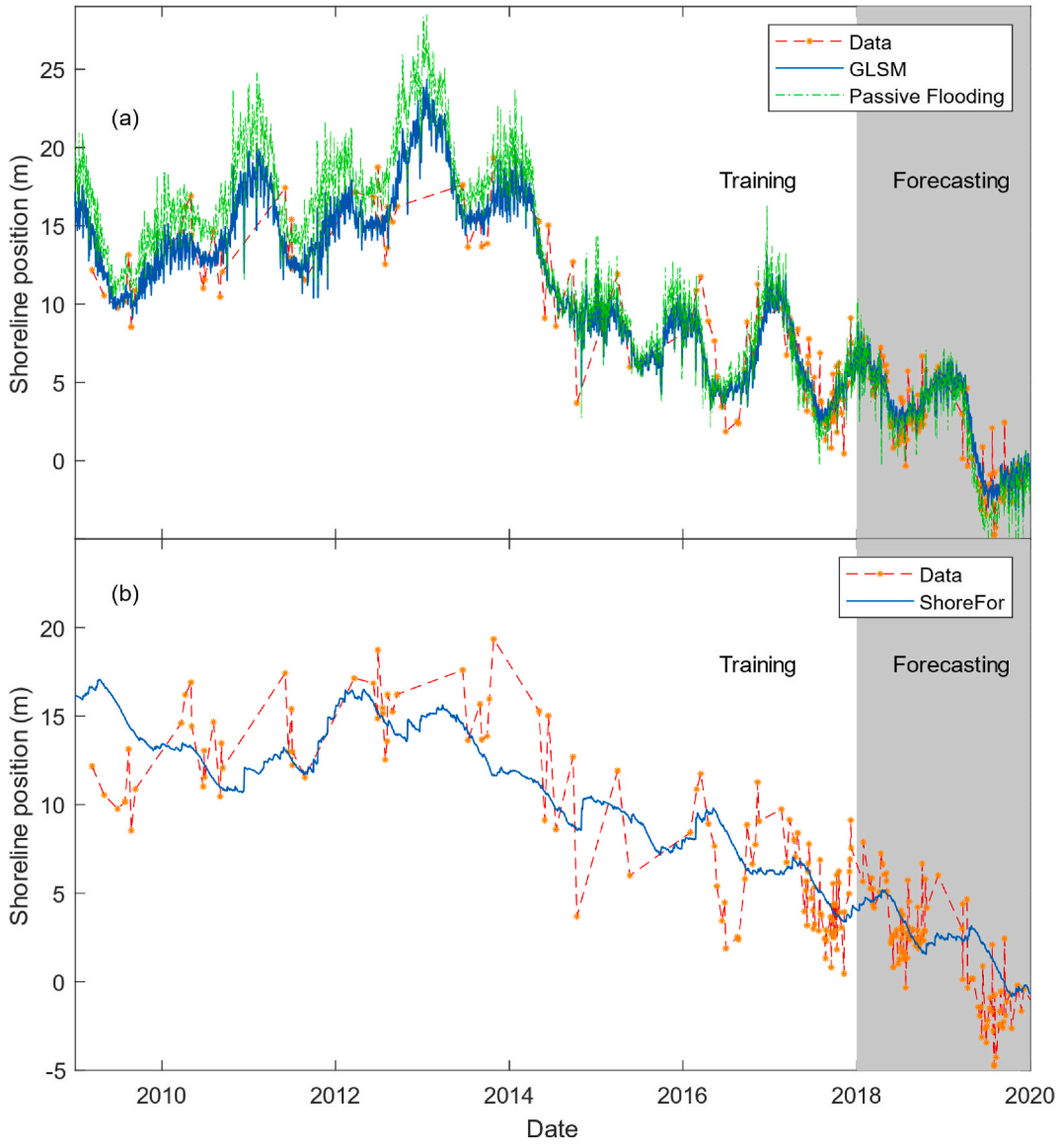

Fig. 8. Jeorse Park Beach model application results. The period 2009–2017 is used for model calibration, and the period 2018–2019 is used for model validation and assessment. Panel (a) shows the results of the GLSM and the passive flooding with $C_{pf} = 1$ while panel (b) shows the results of the ShoreFor model.

Table 2
Calibrated coefficients of the models used for Jeorse Park Beach and West Beach case studies.

Parameters	Jeorse Park Beach	West Beach
GLSM		
C_H ($m^{1.5}/day^{-1}/W^{-0.5}$)	6.22×10^{-8}	5.47×10^{-8}
C_S ($m^{1.5}/day^{-1}/W^{-0.5}$)	2.50×10^{-4}	3.53×10^{-4}
φ_S (days)	132	278
φ_H (days)	5	5
b (m/day)	−0.0005	0.0021
C_{pf}	0.623	0.95
r	0.6319	1.073
ShoreFor		
C ($m^{1.5}/day^{-1}/W^{-0.5}$)	−0.0019	−0.0041
b (m/day)	−0.0055	−0.014
φ (days)	1,570	2,000
r	0.1387	0.1325
Passive Flooding		
C_{pf}	1.08	2.18

Table 3
Skill metrics for GLSM and ShoreFor mode for Jeorse Park Beach. Values without brackets are for the hindcast (calibration) period, and values in brackets correspond to the forecast period.

Skill Metrics	GLSM	ShoreFor	Passive Flooding
RMSE (m)	1.85 (1.5)	2.72 (2.47)	1.92 (1.48)
BSS (improvement over linear trend)	0.66, good (0.78, good)	0.27, poor (0.40, fair)	0.64, good (0.78, good)
BSS (improvement over ShoreFor)	0.53, good (0.63, good)	N/A	0.50, good (0.64, good)
BSS (improvement over Passive Flooding)	0.067, poor (−0.0208, no improvement)	−1.01, no improvement (−1.76, no improvement)	N/A

Table 4
Skill metrics for GLSM and ShoreFor mode for West Beach. Values without brackets are for the hindcast (calibration) period, and values in brackets correspond to the forecast period.

	GLSM	ShoreFor	Passive Flooding
RMSE (m)	2.37 (2.35)	4.41 (4.43)	3.06 (2.69)
BSS (improvement over linear trend)	0.84, excellent (0.74, good)	0.46, fair (0.078, poor)	0.73, good (0.66, good)
BSS (improvement over ShoreFor)	0.71, good (0.72, good)	N/A	0.51, good (0.61, good)
BSS (improvement over Passive Flooding)	0.40, fair (0.24, poor)	−1.055, no improvement (−1.59, no improvement)	N/A

To try and test the model over a much wider range of water level and wave conditions, a hindcast was performed for West Beach with the models for the period 1980–2019, using data from the 2009–2017 period for calibration. To supplement the high-resolution satellite imagery used to calibrate and validate the model between 2009 and 2019, several high-resolution aerial and satellite images from 1987 to 2009 were collected for West Beach and the corresponding shoreline positions were manually calculated and added as points in a longer time series. Long-term model runs were then conducted using the GLSM, passive flooding (only), and ShoreFor models.

The longer-term simulation results are shown in Fig. 10, with comparison statistics provided in Table 5. The GLSM is seen to simulate the shoreline position variability for the entire 40-year period, with excellent improvement over the other models. The GLSM model error is 5.6 m over the 40-year period, during which the total shoreline excursion was nearly 65 m. The ShoreFor model is seen to diverge strongly from the observations over longer timescales, which is due to the fact that the model was calibrated with a period of decreasing water levels (2009–2018) during which the shoreline recessed continuously, and has no knowledge of the water level or how shoreline response is impacted by changing water levels.

The passive flooding model produces a long-term simulation that is more constrained, with better accuracy than ShoreFor, but the passive flooding model is fated to generate only one shoreline position for a given water level, and lacks the ability to replicate wave-enhanced

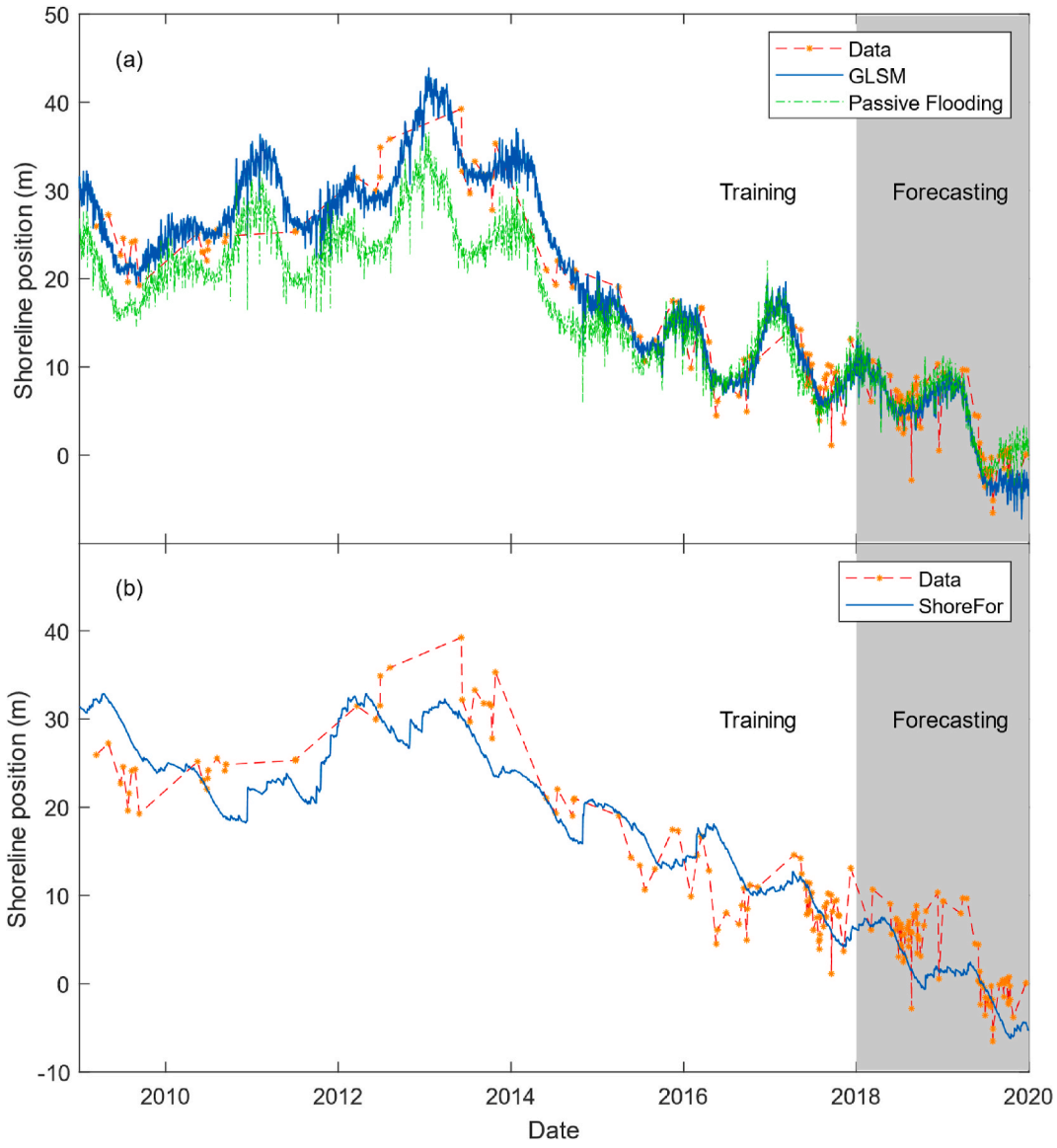

Fig. 9. West Park Beach model application results. The period 2009–2017 is used for model calibration, and the period 2018–2019 is used for model validation and assessment. Panel (a) shows the results of the GLSM and the passive flooding with $C_{pf} = 1$ while panel (b) shows the results of the ShoreFor model.

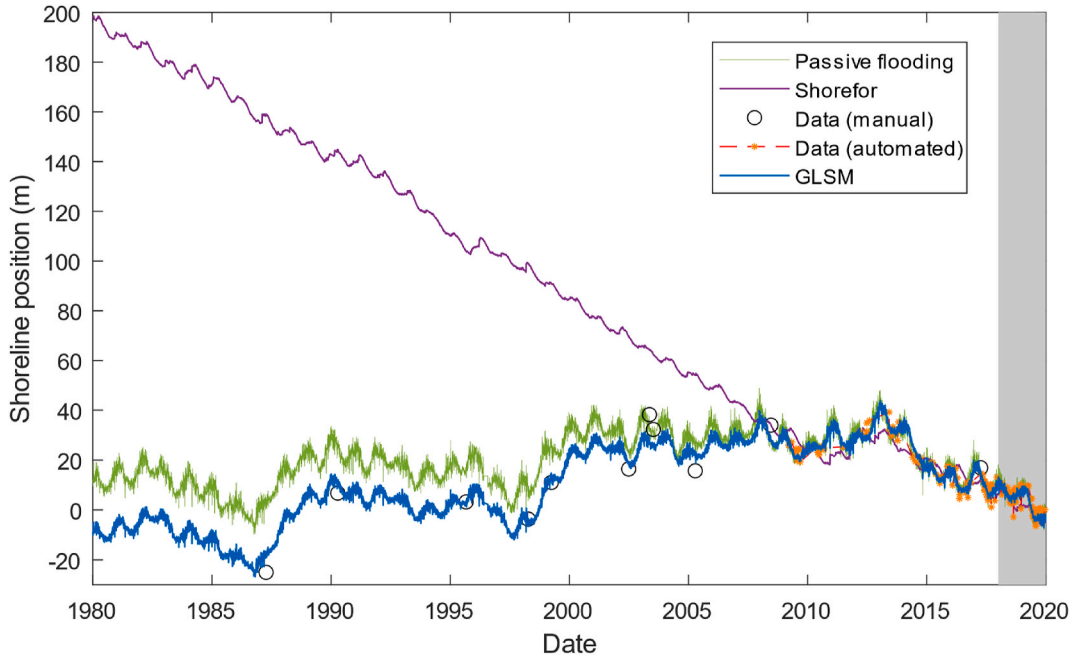

Fig. 10. Comparison between calibrated GLSM, Shorefor, and Passive Flooding Models for the longer time series from 1980 to 2020. The period 2009–2017 was used for model calibration, with hindcast and forecast simulations performed outside this time period (1980–2009 and 2017–2019, respectively). The gray-shaded area represents the forecasting period.

Table 5
Skill metrics for GLSM and ShoreFor models for West Beach for the longer-term simulations from 1980 to 2009.

	GLSM	ShoreFor	Passive flooding
RMSE (m)	5.55	89.03	13.88
BSS (improvement over linear trend)	0.99, excellent	−2.05, no improvement	0.92, excellent
BSS (improvement over ShoreFor)	0.99, excellent	N/A	0.975, excellent
BSS (improvement over Passive Flooding)	0.84, excellent	−39.58, no improvement	N/A

shoreline change or temporal asymmetry in the shoreline position between falling and raising water levels.

Taken in sum, the comparison simulations for the nearly 40-year period suggest that the proposed GLSM, when calibrated, is able to successfully capture water level-enhanced shoreline change, which is arguably the primary mechanism causing shoreline changes for the Great Lakes beaches examined herein.

As is the case for all calibrated, reduced complexity models, care must be taken in interpreting results of good agreement between the model simulation and observation. It should be noted that with the inclusion of the water level disequilibrium and passive flooding terms in the GLSM, three new model parameters are introduced ($C_S, C_{pf},$ and φ_S). These additional constants provide additional degrees of freedom through which the model is calibrated. However, the non-physical calibration parameters for the ShoreFor model when trying to simulate water level effects suggest that additional complexity is needed.

Calibrated simulation parameters show greatly different shoreline response timescales for the wave and water level disequilibrium mechanisms (φ_H *and* φ_S respectively; Table 2). The calibrated wave disequilibrium timescale ($\varphi_H = 5$ days for both beaches) was found to be much shorter than the water level disequilibrium timescales ($\varphi_S =$ 132 and 278 days). To understand these differences, it is important to note that in the limit of the disequilibrium timescale becoming zero, the mechanism shuts down entirely and as there is no disequilibrium to enhance wave-driven shoreline change (e.g. $A = A_{eq}$ in Equation (4)). Thus, the low wave disequilibrium timescales of 5 days suggests that wave disequilibrium plays a negligible role relative to water level disequilibrium for both beaches. The lower value of water level disequilibrium timescale for Jeorse Beach relative to West Beach may be due to the increased importance of the passive flooding mechanism for Jeorse Beach (see Fig. 8); for passive flooding, the timescale of shoreline response is essentially instantaneous.

The low calibration values of the wave disequilibrium timescales (φ_H) and wave forcing coefficients (C_H) relative to the corresponding water level disequilibrium coefficients (φ_S and C_S) suggest that it is water level disequilibrium, not wave disequilibrium, that is most important for wave-driven shoreline changes at these two beaches for the periods investigated.

Differences exist in the depths and shore proximities of the two wave forcing stations used to drive the model for the beaches. These differences make it difficult to extrapolate the model coefficients from this first study beyond these sites, and comparisons of coefficients between the two sites should be carried out with caution. The wave data used in the two case studies are extracted from WIS stations 94001 and 94005, which have different depths of 17 and 11 m respectively. While most of the waves at these stations are deep-water waves due to the relatively low wave periods in Lake Michigan, some of the larger waves are intermediate waves and are affected by the water depth. In any reduced-complexity shoreline model driven by offshore waves, wave transformation effects are site-specific and aliased into model coefficients, so this effect is unavoidable. Additionally, the direct use of station 94005 for the Jeorse Beach simulations does not account for the sheltering effect from Indiana Harbor (Fig. 5) on the wave heights at Jeorse beach. This sheltering effect was absorbed in the model parameters during the calibration process. Obtaining comparable model parameters for different sites would require accounting for the sheltering effect in the input wave data instead of the model parameters. In that regard, more future work needs to be done to address these challenges to standardize wave forcing between different sites, which will in turn allow for the extrapolation and generalization of model coefficients that can be transferred to other sites.

It should be noted that the model accuracy for the two case studies (Tables 3 and 4), shoreline measurements and seasonal variability for the shoreline position all have similar values of approximately 5 m. Therefore, it is difficult to use the current shoreline measurement data to infer the seasonal variability in the shoreline position and to validate the seasonal variability shown by the model simulations using the available data. In essence, on short timescales over which the shoreline movement is small, it is hard to attribute the differences between the model simulation and the measurement to the lack of model skill. Even though the shoreline positions inferred herein are leveraging the most accurate and high-resolution satellite imagery available at present, future work could involve model testing with even more accurate shoreline position datasets, derived by in-situ imaging or field surveys.

6. Conclusions

In this paper, a new shoreline evolution model, the Great Lakes Shoreline Model (GLSM), was developed and tested. Motivated by recent large water level fluctuations in the Great Lakes, this model was developed in response to the need for a reduced-complexity shoreline model that can successfully account for the influence of large seasonal and interannual water level fluctuations on shoreline changes. Building on the structure of existing reduced-complexity shoreline models such as ShoreFor (Splinter et al., 2014) and CoSMoS-COAST (Vitousek et al., 2017), the proposed model assumes that wave-forced shoreline changes are modulated by the summed water level and wave disequilibrium, with additional terms for passive flooding/exposure and unresolved processes. Simple case studies demonstrate the ability of the model to generate shoreline changes consistent with seasonal and interannual patterns of waves and water levels as seen in the Great Lakes.

The model was applied to two sandy sites in southern Lake Michigan with different wave characteristics. Calibration and validation shoreline position time series were obtained from high resolution commercial satellite images, Planetscope and RapidEye. The GLSM was compared to the ShoreFor model, which is not formulated to account for water level effects, as well as a simple passive flooding/exposure model for which shoreline change is proportional to the beach face slope. For a nine-year period during which the water level consistently rose, the GLSM model hindcasts and forecasts showed improvement over both models, with more substantial improvement over both models for the beach with greater wave forcing (West Beach).

The application of the models to a Lake Michigan beach over a nearly forty-year period of highly-variable water levels and shoreline position highlights the true potential improvement provided by the proposed model. The GLSM was able to simulate the shoreline position with RMSE of less than 5 m, whereas the comparison models showed extensive long-term drift due to the aliasing of water level effects into other terms.

More applications of the model are needed to better understand and improve the model for a wider range of coastal conditions. The model formulation raises numerous questions about shoreline responses to coastal hydrodynamic processes, and the investigation of these questions may provide insight to coastal responses to sea level rise. To date, reduced complexity shoreline models attempting to account for sea level rise operate on two extremes of the temporal spectrum – either short-term passive flooding, or long-term equilibration via the Bruun Rule. The model described herein affords a tunable, intermediate timescale (φ_S) that can potentially bridge the gap between these two extremes, which may allow more accurate intermediate predictions of the effects of sea level rise for ocean coasts.

Finally, it is hoped that this model paves the road for the improved predication of shoreline positions in the Great Lakes, which motivated the model development, in turn aiding in the design of coastal measures along Great Lakes shorelines to better buffer the large interannual water level fluctuations that have recently caused widespread damage to shoreline communities.

CRediT authorship contribution statement

Hazem U. Abdelhady: Conceptualization, Data curation, Formal analysis, Investigation, Methodology, Software, Writing – original draft, Writing – review & editing. **Cary D. Troy:** Conceptualization, Formal analysis, Investigation, Methodology, Funding acquisition, Project administration, Resources, Supervision, Validation, Writing – original draft, Writing – review & editing.

Declaration of competing interest

The authors declare that they have no known competing financial interests or personal relationships that could have appeared to influence the work reported in this paper.

Data availability

Data will be made available on request.

Acknowledgements

This work was supported in part by the Illinois-Indiana Sea Grant College Program, grant number NA18OAR4170082, and the Indiana Department of Natural Resources Lake Michigan Coastal Program, grant number NA20NOS4190036. The authors are grateful to Bob Jensen from the United States Army Corps of Engineers for providing WIS wave model output. We acknowledge the use of imagery from the Smallsat Data Explore application (https://csdap.earthdata.nasa.gov), part of the NASA Commercial Smallsat Data Acquisition Program.

References

Abdelhady, H.U., Troy, C.D., Habib, A., Manish, R., 2022. A simple, fully automated shoreline detection algorithm for high-resolution multi-spectral imagery. Rem. Sens. 14, 557. https://doi.org/10.3390/rs14030557.

Alauddin Al Azad, A.S.M., Mita, K.S., Zaman, M.W., Akter, M., Asik, T.Z., Haque, A., Hussain, M.A., Rahman, M.M., 2018. Impact of tidal phase on inundation and thrust force due to storm surge. J. Mar. Sci. Eng. 6, 110. https://doi.org/10.3390/JMSE6040110, 6 (2018) 110.

Antolínez, J.A.A., Méndez, F.J., Anderson, D., Ruggiero, P., Kaminsky, G.M., 2019. Predicting climate-driven coastlines with a simple and efficient multiscale model. J. Geophys. Res. Earth Surf. 124, 1596–1624. https://doi.org/10.1029/2018JF004790.

Ashton, A.D., Murray, A.B., 2006. High-angle wave instability and emergent shoreline shapes: 1. Modeling of sand waves, flying spits, and capes. J. Geophys. Res. Earth Surf. 111, 4011. https://doi.org/10.1029/2005JF000422.

Athanasiou, P., van Dongeren, A., Giardino, A., Vousdoukas, M., Gaytan-Aguilar, S., Ranasinghe, R., 2019. Global distribution of nearshore slopes with implications for coastal retreat. Earth Syst. Sci. Data 11, 1515–1529. https://doi.org/10.5194/ESSD-11-1515-2019.

Bockheim, J.G., 2020. Soils of the Laurentian Great Lakes, USA and Canada. Springer Nature, pp. 99–109.

Bruun, P., 1962. Sea-level rise as a cause of shore erosion. J. Waterw. Harb. Div. 88, 117–130. https://doi.org/10.1061/JWHEAU.0000252.

Cheng, V.Y.S., Saber, A., Alberto Arnillas, C., Javed, A., Richards, A., Arhonditsis, G.B., 2021. Effects of hydrological forcing on short- and long-term water level fluctuations in Lake Huron-Michigan: a continuous wavelet analysis. J. Hydrol. (Amst.) 603, 127164. https://doi.org/10.1016/j.jhydrol.2021.127164.

Coco, G., Senechal, N., Rejas, A., Bryan, K.R., Capo, S., Parisot, J.P., Brown, J.A., MacMahan, J.H.M., 2014. Beach response to a sequence of extreme storms. Geomorphology 204, 493–501. https://doi.org/10.1016/J.GEOMORPH.2013.08.028.

Davidson, M.A., Splinter, K.D., Turner, I.L., 2013. A simple equilibrium model for predicting shoreline change. Coast. Eng. 73, 191–202. https://doi.org/10.1016/j.coastaleng.2012.11.002.

Deep, K., Singh, K.P., Kansal, M.L., Mohan, C., 2009. A real coded genetic algorithm for solving integer and mixed integer optimization problems. Appl. Math. Comput. 212, 505–518. https://doi.org/10.1016/J.AMC.2009.02.044.

D'anna, M., Idier, D., Castelle, B., Vitousek, S., le Cozannet, G., 2021. Reinterpreting the Bruun Rule in the context of equilibrium shoreline models. J. Mar. Sci. Eng. 9, 974. https://doi.org/10.3390/JMSE9090974.

Feng, X., Ma, G., Su, S.F., Huang, C., Boswell, M.K., Xue, P., 2020. A multi-layer perceptron approach for accelerated wave forecasting in Lake Michigan. Ocean Eng. 211, 107526 https://doi.org/10.1016/J.OCEANENG.2020.107526.

Friedrichs, C.T., 2011. Tidal flat morphodynamics: a synthesis, treatise on estuarine and coastal. Science 3, 137–170.

Gronewold, A.D., Rood, R.B., 2019. Recent water level changes across Earth's largest lake system and implications for future variability. J. Great Lake. Res. 45, 1–3. https://doi.org/10.1016/J.JGLR.2018.10.012.
Hanrahan, J.L., Kravtsov, S.v., Roebber, P.J., 2009. Quasi-periodic decadal cycles in levels of lakes Michigan and Huron. J. Great Lake. Res. 35, 30–35. https://doi.org/10.1016/j.jglr.2008.11.004.
Hanson, H., 1989. GENESIS - a generalized shoreline change numerical model. J. Coast Res. 5, 1–27.
Ibaceta, R., Splinter, K.D., Harley, M.D., Turner, I.L., 2020. Enhanced coastal shoreline modeling using an ensemble kalman filter to include nonstationarity in future wave climates. Geophys. Res. Lett. 47 https://doi.org/10.1029/2020GL090724.
Katoch, S., Chauhan, S.S., Kumar, V., 2021. A review on genetic algorithm: past, present, and future. Multimed. Tool. Appl. 80, 8091–8126. https://doi.org/10.1007/S11042-020-10139-6/FIGURES/8.
Lesser, G.R., Roelvink, J.A., van Kester, J.A.T.M., Stelling, G.S., 2004. Development and validation of a three-dimensional morphological model. Coast. Eng. 51, 883–915. https://doi.org/10.1016/J.COASTALENG.2004.07.014.
Masselink, G., Short, A.D., 1993. The Effect of tide range on beach morphodynamics and morphology: a conceptual beach model. J. Coast Res. 785–800.
MATLAB, 9.10.0.1602886 (R2020a), 2019. The MathWorks Inc., Natick, Massachusetts.
Melby, J.A., Nadal-Caraballo, N.C., Pagan-Albelo, Y., Ebersole, B., 2012. Wave height and water level variability on lakes Michigan and St Clair. Engineer Research and Development Center Vicksburg Ms Coastal and Hydraulics Lab.
Miller, J.K., Dean, R.G., 2004. A simple new shoreline change model. Coast. Eng. 51, 531–556. https://doi.org/10.1016/j.coastaleng.2004.05.006.
Mortimer, C.H., 2004. Lake Michigan in motion: responses of an inland sea to weather, earth-spin, and human activities. Univ of Wisconsin Press.
Muir, F.M.E., Hurst, M.D., Vitousek, S., Hansom, J.D., Rennie, A.F., Fitton, J.M., Naylor, L.A., 2020. Predicting coastal change in scotland across decadal-centennial timescales using a process-driven one-line model. ICE Publishing, pp. 551–563.
Pape, L., Kuriyama, Y., Ruessink, B.G., 2010. Models and scales for cross-shore sandbar migration. J. Geophys. Res. Earth Surf. 115, 3043. https://doi.org/10.1029/2009JF001644.
Payo, A., Hall, J.W., French, J., Sutherland, J., van Maanen, B., Nicholls, R.J., Reeve, D. E., 2016. Causal loop analysis of coastal geomorphological systems. Geomorphology 256, 36–48. https://doi.org/10.1016/J.GEOMORPH.2015.07.048.
Robinet, A., Castelle, B., Marieu, V., Splinter, K.D., Harley, M.D., 2017. On a reduced-complexity shoreline model combining cross-shore and alongshore processes. Coast. Dynam. https://doi.org/10.1016/j.envsoft.2018.08.010.
Robinet, A., Idier, D., Castelle, B., Marieu, V., 2018. A reduced-complexity shoreline change model combining longshore and cross-shore processes: the LX-Shore model. Environ. Model. Software 109, 1–16. https://doi.org/10.1016/J.ENVSOFT.2018.08.010.
Roelvink, D., Reniers, A., van Dongeren, A., van Thiel de Vries, J., McCall, R., Lescinski, J., 2009. Modelling storm impacts on beaches, dunes and barrier islands. Coast. Eng. 56, 1133–1152. https://doi.org/10.1016/J.COASTALENG.2009.08.006.
Schepper, R., Almar, R., Bergsma, E., de Vries, S., Reniers, A., Davidson, M., Splinter, K., 2021. Modelling cross-shore shoreline change on multiple timescales and their interactions. J. Mar. Sci. Eng. 9, 582. https://doi.org/10.3390/JMSE9060582.
Splinter, K.D., Turner, I.L., Davidson, M.A., Barnard, P., Castelle, B., Oltman-Shay, J., 2014. A generalized equilibrium model for predicting daily to interannual shoreline response. J. Geophys. Res. Earth Surf. 119, 1936–1958. https://doi.org/10.1002/2014JF003106.
Sutherland, J., Soulsby, R.L., 2003. Use of model performance statistics in modelling coastal morphodynamics. In: Proceedings of the International Conference on Coastal Sediments, pp. 1–14.
Team, P.. Planet application program interface, Space for Life on Earth, (n.d.). https://api.planet.com.
Theuerkauf, E.J., Braun, K.N., Nelson, D.M., Kaplan, M., Vivirito, S., Williams, J.D., 2019. Coastal geomorphic response to seasonal water-level rise in the laurentian Great lakes: an example from Illinois beach state Park, USA. J. Great Lake. Res. 45, 1055–1068.
Thompson, T.A., Baedke, S.J., 1995. Beach-ridge development in Lake Michigan: shoreline behavior in response to quasi-periodic lake-level events. Mar. Geol. 129, 163–174. https://doi.org/10.1016/0025-3227(95)00110-7.
Tran, Y.H., Barthélemy, E., 2020. Combined longshore and cross-shore shoreline model for closed embayed beaches. Coast. Eng. 158, 103692 https://doi.org/10.1016/j.coastaleng.2020.103692.
Troy, C.D., Cheng, Y.-T., Lin, Y.-C., Habib, A., 2021. Rapid lake Michigan shoreline changes revealed by UAV LiDAR surveys. Coast. Eng. 170, 104008 https://doi.org/10.1016/J.COASTALENG.2021.104008.
U.S. Army Corps of Engineers, 2022. Wave Information Studies. http://wis.usace.army.mil/. (Accessed 1 October 2022).
Vitousek, S., Barnard, P.L., 2015. A nonlinear, implicit one-line model to predict long-term shoreline change. World Scientific Pub Co Pte Lt.
Vitousek, S., Barnard, P.L., Limber, P., Erikson, L., Cole, B., 2017. A model integrating longshore and cross-shore processes for predicting long-term shoreline response to climate change. J. Geophys. Res. Earth Surf. 122, 782–806. https://doi.org/10.1002/2016JF004065.
Wright, L.D., Short, A.D., 1984. Morphodynamic variability of surf zones and beaches: a synthesis. Mar. Geol. 56, 93–118. https://doi.org/10.1016/0025-3227(84)90008-2.
Yates, M.L., Guza, R.T., O'Reilly, W.C., 2009. Equilibrium shoreline response: observations and modeling. J. Geophys. Res. Oceans 114. https://doi.org/10.1029/2009JC005359.